

## A Gaussian-2 Quantum Chemical Study of CHNO: Isomerization and Molecular Dissociation Reactions

Warwick A. Shapley<sup>†</sup> and George B. Bacskay\*

School of Chemistry, The University of Sydney, NSW, 2006, Australia

Received: January 25, 1999; In Final Form: June 8, 1999

The results of an ab initio quantum chemical study, carried out at the Gaussian-2 (G2) level of theory, of the potential energy surface governing the isomerization and dissociation reactions of the CHNO isomers (to CH + NO, NH + CO, and OH + CN) are reported. In general, several pathways were found that interconnect each open-chain or cyclic isomer with the others. In particular, two bifurcation points were located; the first connects HCNO to both HNCO and cyclic N(H)CO, the second connects HOCN to HNCO and cyclic N(H)-CO. The lowest energy pathways for the isomerization of the open-chain species are two-step reactions that proceed via cyclic intermediates. Comparison of the G2 energies with those obtained in density functional (DFT) and QCISD(T)/cc-pVTZ calculations show a reasonable level of consistency, although differences up to ~9 kcal/mol were found between G2 and DFT.

### Introduction

The isomers of CHNO have been extensively studied for a number of reasons, not least because they are the simplest “organic” molecules containing the elements carbon, hydrogen, nitrogen, and oxygen.<sup>1–5</sup> The most stable isomers are the open-chain species HNCO (isocyanic acid), HCNO (fulminic acid), HONC (isofulminic acid), and HOCN (cyanic acid), although some ring isomers also exist as stable intermediates. These compounds play an important role in N-containing fuel chemistry because they are formed through the initial step of “reburning”<sup>6–10</sup> of methylenide (CH) with NO, a reaction that can be utilized to reduce the amount of nitric oxides (NO<sub>x</sub>) emitted from combustion exhausts. In a different vein, isocyanic acid is used as the active species in the “RAPRENO<sub>x</sub>” NO<sub>x</sub> abatement process.<sup>11</sup> Here, cyanuric acid (HOCN)<sub>3</sub> is injected into exhaust streams, whereupon it decomposes to HNCO which then undergoes a series of reactions resulting in NO<sub>x</sub> destruction. In addition to being formed directly from CH and NO, HCNO is produced by the dissociation of the formaldiminoxy radical (CH<sub>2</sub>NO) which itself is formed by the association of CH<sub>2</sub> with NO.<sup>12–14</sup> Loss of a H atom has been demonstrated<sup>15</sup> to be one of the dominant reactions undergone by CH<sub>2</sub>NO and thus it acts as another source of CHNO species in combustion systems.

The isomers of CHNO play an important role in the combustion chemistry of N-containing compounds and the successful modeling of such systems requires accurate mechanistic and thermodynamic data for the isomerization and dissociation reactions of these species. In previous studies<sup>12,16,17</sup> we explored the reactions of CH<sub>2</sub>NO using G2 theory,<sup>18</sup> which was found to perform well for this system when compared with CASPT2, QCISD(T), and CCSD(T) calculations carried out in conjunction with the cc-pVTZ basis of Dunning et al.<sup>19</sup> The present paper represents a continuation of that work by examining the G2 potential energy surface (PES) of the CHNO system. A systematic study of both the singlet and triplet states of the CHNO system was recently carried out by Mebel et al.<sup>1</sup>

at the B3LYP/6-311G(d,p) level of density functional theory (DFT) and therefore it is of some interest to compare their results with ab initio data such as the G2 results reported in this paper. In general we find that although the G2 relative energies for isomers and transition states are in reasonable agreement with the DFT results, differences up to ~9 kcal/mol do occur. This has prompted a further, more detailed investigation as to the relative accuracy of the G2 and DFT approaches, by computing the energies of selected species at the QCISD(T)/cc-pVTZ and B3LYP/cc-pVTZ levels of theory as well. Furthermore, because several fairly obvious reaction pathways were not considered by Mebel et al., the characterization of these is also part of this study.

### Computational Methods

All stationary points on the PES were characterized in accordance with the G2 procedure<sup>18</sup> by optimizing molecular geometries initially at the HF/6-31G(d) level, at which point zero-point energies were also calculated using vibrational frequencies scaled by the recommended factor of 0.893. The higher level and larger basis computations were then carried out at geometries reoptimized at the MP2/6-31G(d) level. Species with singlet electronic states were computed using the spin-restricted Hartree-Fock and Møller-Plesset perturbation formalisms RHF and RMP $n$ ; those with triplet electronic states were computed using the unrestricted formalisms UHF and UMP $n$ . G2 aims at reproducing essentially a QCISD(T)/6-311+G(3df,2p) energy and further corrects this with an empirical higher level correction (HLC). The final G2 energies include the zero point energy (ZPE) so that differences in G2 energies between two species are equivalent to differences in their enthalpies (and free energies) of formation at 0 K. For selected species the energies were also computed at the QCISD(T)/cc-pVTZ, B3LYP/cc-pVTZ, and B3LYP/6-311G(d,p) levels of theory so as to elucidate the origin of any discrepancy between the current G2 results and the B3LYP results of Mebel et al.<sup>1</sup> All calculations were performed using the Gaussian 94 system of programs,<sup>20</sup> unless otherwise indicated.

\* Corresponding author.

<sup>†</sup> Current address: Department of Chemistry, University of British Columbia, Vancouver, B.C., V6T 1Z1, Canada.

**TABLE 1: G2 Total and Zero-Point Vibrational, and G2 and B3LYP Relative (to HCNO) Energies of Isomers and Transition States Associated with the Isomerization and Dissociation Reactions of HCNO<sup>a</sup>**

	G2 <sup>b</sup> ( $E_h$ )	$\Delta E_{ZPE}(G2)$ (kcal/mol)	G2 relative energy (kcal/mol)	B3LYP/6-311G(d,p) relative energy <sup>c</sup> (kcal/mol)
HCNO ( <sup>1</sup> A')	-168.345058	12.88	0.00	0.0
TS1 ( <sup>1</sup> A') <sup>d</sup>	-168.222480	8.46	76.9	
HONC ( <sup>1</sup> A')	-168.323159	12.57	13.7	19.2
TS2 ( <sup>1</sup> A')	-168.228487	10.26	73.2	69.8
Cyclic C(H)NO ( <sup>1</sup> A') <sup>d</sup>	-168.321555	11.71	14.8	24.0
NC(H)O ( <sup>3</sup> A'')	-168.316895	11.31	17.7	14.7 <sup>e</sup>
NC(H)O ( <sup>3</sup> A')	-168.293203	11.47	32.5	27.2 <sup>e</sup>
Cyclic C(H)NO ( <sup>3</sup> A)	-168.239193	11.93	66.4	65.6
TS3 ( <sup>1</sup> A')	-168.238651	10.88	67.4	
HNCO ( <sup>1</sup> A')	-168.456771	12.77	-70.1	-67.9
HNCO ( <sup>3</sup> A)	-168.316791	10.96	17.7	14.7
Cyclic N(H)CO ( <sup>1</sup> A)	-168.287896	12.26	35.9	44.4
CN(H)O ( <sup>3</sup> A'')	-168.208470	11.81	85.7	80.1
TS4 ( <sup>1</sup> A')	-168.237367	8.88	67.6	77.4
TS5 ( <sup>1</sup> A') <sup>d</sup>	-168.283411	10.29	38.7	
Cyclic O(H)CN ( <sup>1</sup> A') <sup>d</sup>	-168.283500	10.99	38.6	
TS6 ( <sup>1</sup> A)	-168.279369	10.98	41.2	
HOCN ( <sup>1</sup> A')	-168.416250	13.18	-44.7	-39.2
HOCN ( <sup>3</sup> A)	-168.275565	11.98	43.6	
TS7 ( <sup>1</sup> A') <sup>d</sup>	-168.273829	9.99	44.7	
TS8 ( <sup>1</sup> A)	-168.265174	10.13	50.1	55.8
TS9 ( <sup>1</sup> A')	-168.316590	9.47	17.9	
TS10 ( <sup>1</sup> A')	-168.233722	8.13	69.9	78.0
TS11 ( <sup>1</sup> A') <sup>d</sup>	-168.153771	7.65	120.0	
TS12 ( <sup>3</sup> A'')	-168.303083	9.70	26.3	24.8
SC1 ( <sup>3</sup> A'')	-168.311347	12.34	20.1	17.9
TS13 ( <sup>1</sup> A') <sup>d</sup>	-168.243653	7.92	63.6	
HC ( <sup>2</sup> II) + NO ( <sup>2</sup> II)	-168.15253	10.74	120.8	122.8
HN ( <sup>3</sup> $\Sigma$ ) + CO ( <sup>1</sup> $\Sigma$ )	-168.31966	12.14	15.9	20.4
HN ( <sup>1</sup> $\Delta$ ) + CO ( <sup>1</sup> $\Sigma$ )	-168.255142	9.56	56.4	
HO ( <sup>2</sup> II) + CN ( <sup>2</sup> $\Sigma$ )	-168.22667	12.16	74.3	78.7
HNOC ( <sup>1</sup> A') <sup>d</sup>	-168.246273	10.07	62.0	67.1
HCON ( <sup>1</sup> A')	-168.216877	9.98	80.4	

<sup>a</sup> At MP2/6-31G(d) geometry unless stated otherwise. <sup>b</sup> G2 energy includes the zero-point correction  $\Delta E_{ZPE}(G2)$ . <sup>c</sup> Results of Mebel et al.<sup>1</sup> unless indicated otherwise. <sup>d</sup> Using scaled MP2 frequencies. <sup>e</sup> Obtained in this work.

## Results and Discussion

The G2 energies of all isomers and transition states corresponding to stationary points on the CHNO PES are listed in Table 1; energies relative to HCNO (<sup>1</sup>A') are also tabulated along with the corresponding DFT results of Mebel et al.<sup>1</sup> The various isomerization and dissociation pathways available to each isomer are depicted in Figure 1. The MP2/6-31G(d) geometries of the open-chain and ring isomers are given in Figures 2 and 3, respectively, whereas those of transition states are in Figures 4 and 5. All species with closed-shell (<sup>1</sup>A') configurations possess four electrons in a'' molecular orbitals (MO). In general, the singlet state of a given species lies considerably lower in energy than the corresponding triplet, so for most purposes only the former need be considered in the study of reaction mechanisms. The two C-O-N-chain isomers HNOC and HCON lie sufficiently higher in energy (by 62.0 and 80.4 kcal/mol, respectively) than HCNO so as to render them unimportant when considering possible reaction schemes. Consequently, HNOC and HCON do not appear in Figure 1 and will not be discussed further.

As indicated in Figure 1, the open chain isomers HCNO, HONC, HNCO, and HOCN can interconvert by direct, one-step reactions or by the formation of cyclic intermediates, i.e., two-step reactions. Only the latter possibilities concerned Mebel et al.<sup>1</sup>, although the one involving cyclic O(H)CN was not considered. With respect to the dissociation pathways, the current study is restricted to the molecular channels, i.e., producing HC + NO, HN + CO, and HO + CN. The study of

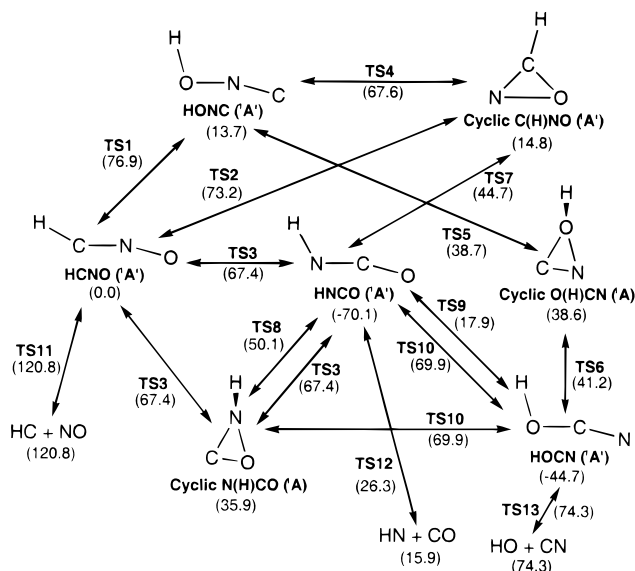


**Figure 1.** Reaction pathways for HCNO isomerizations and dissociations. (The G2 energies in parentheses are relative to HCNO, in kcal/mol.)

Mebel et al. includes also the O + HCN/HNC, C + HNO/HON, N + HCO/HOC, and H + CNO/NCO/cyclic CON channels.

**1. HCNO (<sup>1</sup>A') → HONC (<sup>1</sup>A')/Cyclic C(H)NO (<sup>1</sup>A').** The schematic G2 PES for these reactions is depicted in Figure 6. On the basis of MP2 geometries, fulminic acid (HCNO) exists

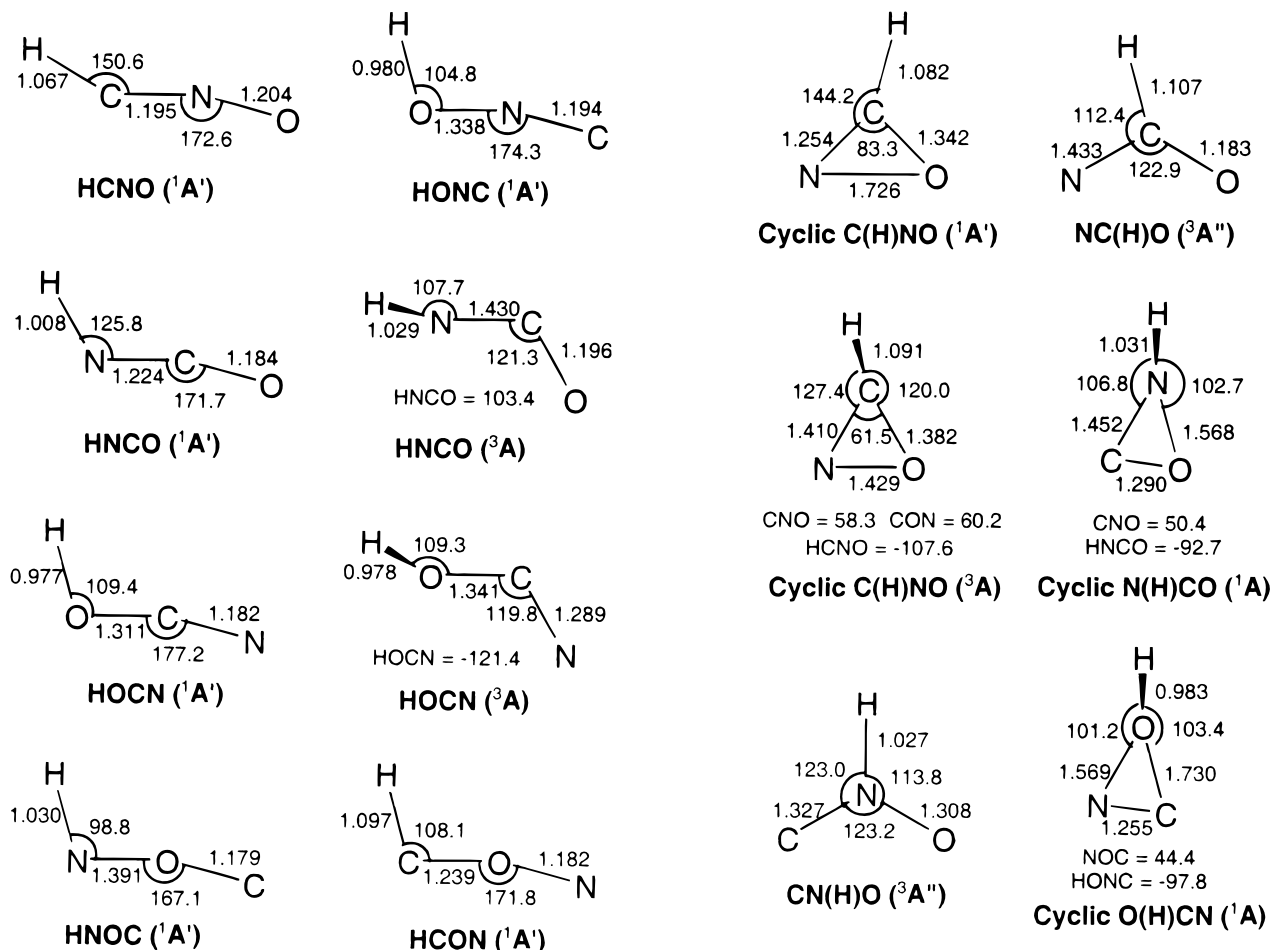


**Figure 2.** MP2/6-31G(d) geometries of species corresponding to stationary points on the PES describing the open-chain HCNO isomers.

as a planar, bent molecule with a ( $^1A'$ ) ground electronic state. The geometry of this molecule has been the subject of quite intensive study in recent years<sup>21,22</sup> because the barrier to linearity is of the order of only a few wavenumbers and thus it is one of only a handful of molecules to exhibit the property of quasi-linearity. Although the MP2 HCN angle of  $151^\circ$  might suggest otherwise, the barrier at this level of theory is also very low at only 0.6 kcal/mol, and in fact at the G2 level this barrier disappears completely with the linear ( $^1\Sigma$ ) form being 0.15 kcal/mol lower in energy than the bent form. The corresponding H-X-Y angles (X, Y = C, N, or O) for the other open-chain isomers are considerably less than the value of  $151^\circ$  obtained for HCNO.

The rearrangement of HCNO to HONC ( $^1A'$ ) can proceed by cyclization followed by H migration and ring opening as considered by Mebel et al.<sup>1</sup>, or by direct 1,3-hydrogen migration from C to O. This latter possibility was not considered by Mebel et al. Throughout the course of the 1,3-H migration the CNO angle remains less than  $180^\circ$ , allowing the H to keep in close contact with the N. Indeed, at the transition state (TS1) the HN length is only 1.09 Å. The H migration could thus be viewed as a pseudo two-step process, involving first a 1,2-H shift from C to N followed by another 1,2-shift from N to O; note that there is a single transition state in the process that effectively corresponds to a CN(H)O molecule. Using the intrinsic reaction coordinate (IRC) approach at the MP2/6-31G(d) level of theory, we confirmed that TS1 connects HCNO and HONC. The normal mode corresponding to the imaginary frequency ( $1703i$  cm $^{-1}$  at the MP2/6-31G(d) level) is of  $a'$  symmetry, as expected, given

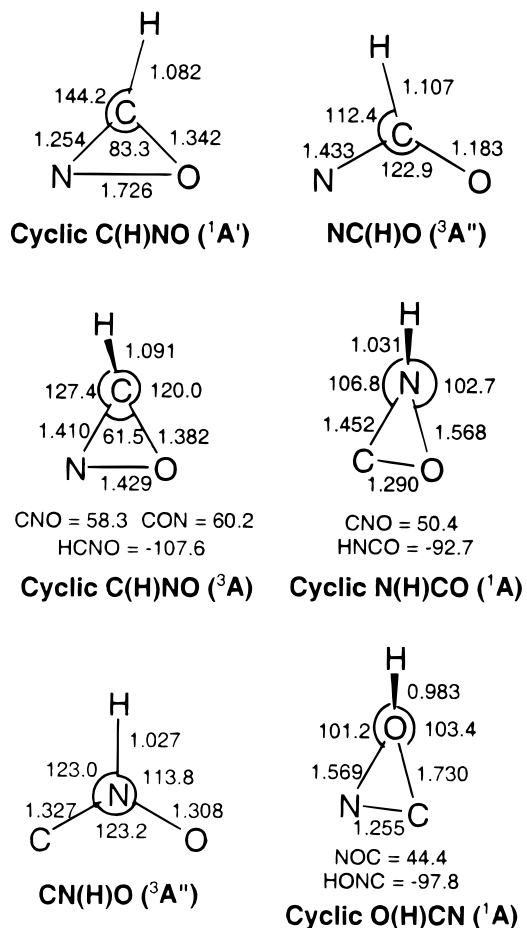


**Figure 3.** MP2/6-31G(d) geometries of species corresponding to stationary points on the PES describing the cyclic and branched HCNO isomers.

that the hydrogen migration takes place in the molecular plane. Note that there appears to be no equilibrium structure corresponding to the  $^1A'$  state of CN(H)O. The barrier height associated with TS1 is 76.9 kcal/mol, which is comparable with the barrier heights for 1,3- and 1,2-H shifts in  $\text{CH}_2\text{NO}$ .<sup>16</sup>

HCNO may also cyclize to cyclic C(H)NO (oxazirine) ( $^1A'$ ) by decreasing the CNO angle, allowing a gradual OC bond formation. At the corresponding transition state (TS2) the NO bond lengthened substantially from 1.20 to 1.44 Å, which in the final product (oxazirine) is 1.73 Å, indicative of a very weak NO bond. (Indeed the open-chain NC(H)O isomer is only  $\sim 3$  kcal/mol higher in energy.) According to G2, the reaction enthalpy of the cyclization process of oxazirine is 14.8 kcal/mol with a (forward) barrier height of 73.2 kcal/mol. The relative stability of cyclic C(H)NO, at least in comparison with the other cyclic structures, may be understood in part by consideration of its Lewis structure; note that it can be drawn such that each atom possesses the "correct" number of bonding and nonbonding electron pairs.

Cyclic C(H)NO appears to possess a low-lying triplet excited state, although given the large NCO angle ( $\sim 123^\circ$ ) and the long NO distance ( $\sim 2.30$  Å), this molecule should really be considered an open-chain species NC(H)O ( $^3A''$ ). According to G2, this state lies 2.9 kcal/mol above the  $^1A'$  state of cyclic C(H)NO. The energy separation of these two states was also studied at the CASPT2/cc-pVTZ and QCISD(T)/cc-pVTZ levels of theory (at CASSCF/cc-pVDZ geometries) in our previous work.<sup>17</sup> In contrast to G2, both of the above methods placed the triplet state *below* the singlet state by 3.5 and 0.7 kcal/mol,

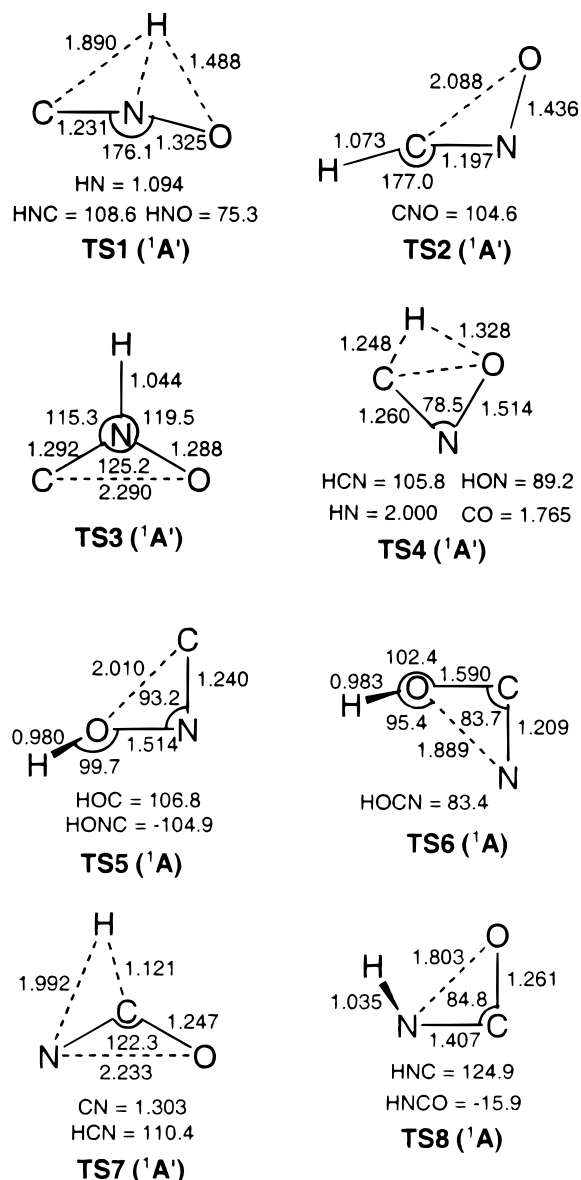


**Figure 4.** MP2/6-31G(d) geometries of species corresponding to stationary points on the PES describing transition states of the HCNO isomers.

respectively. Although reactions taking place on the  $^1A'$  surface would therefore seem to go to an excited state of this molecule, intersystem crossing to the ground (triplet) state would nevertheless be possible, given their near-degenerate energies, with the rate of crossing of course being governed by the degree of spin-orbit coupling.

As indicated above, the ground state of NC(H)O was found to be  $^3A''$ . The lowest excited state of this system is  $^3A'$  that lies 14.87 kcal/mol above the ground state, when computed at the G2 level. These results are in good agreement with the results of our B3LYP/6-311G(d,p) calculations that were carried out in an attempt to resolve an apparent contradiction between our G2 results and the findings of Mebel et al.,<sup>1</sup> who labeled the ground state of NC(H)O as  $^3A'$  and which they found to lie 15.0 kcal/mol above HCNO. It appears that Mebel et al. simply mislabeled their ground state equilibrium structure (which agrees perfectly with what we obtained for the  $^3A''$  state). The small difference in the respective energies relative to HCNO probably stems from the different choices of point group symmetry for HCNO (assumed to be  $C_s$  in our work).

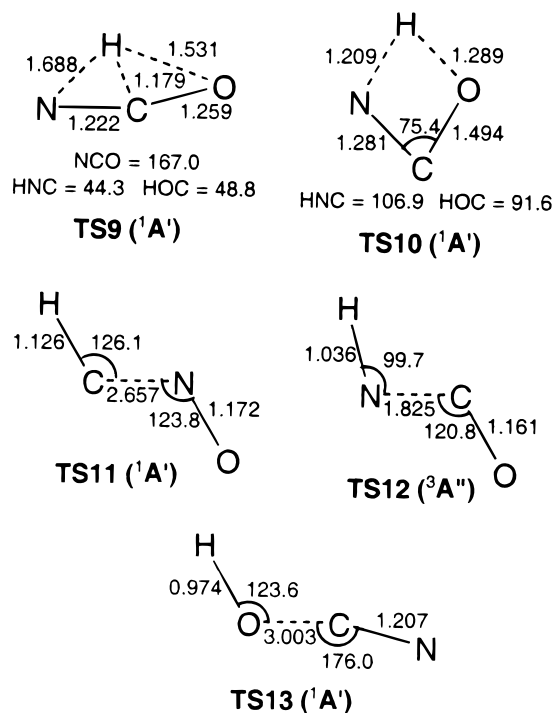


**Figure 5.** MP2/6-31G(d) geometries of species corresponding to stationary points on the PES describing transition states of the HCNO isomers.

**2. HCNO ( $^1A'$ )  $\rightarrow$  HNCO ( $^1A'$ )/Cyclic N(H)CO ( $^1A$ ).** The unusual feature of these two reactions is that both proceed through the *same* transition state (TS3), as indicated in Figure 6. Starting with HCNO, the H atom moves toward N while the CNO angle decreases. At the transition state geometry the HN bond is essentially complete, but commensurate with the CNO angle of  $125^\circ$  an incipient CO bond is evident. TS3 is planar and possesses only one imaginary  $a'$  frequency; all  $a''$  frequencies are real. If the reaction coordinate is followed and hence planarity is maintained, as the CO distance decreases the NO bond lengthens, resulting in HNCO ( $^1A'$ ), which is the most stable of all CHNO isomers. This pathway was not considered by Mebel et al.<sup>1</sup>

There is, however, a portion of the PES on the product side of the reaction coordinate where it is actually a *maximum* with respect to an out-of-plane motion of the H atom, i.e., the molecule has an imaginary  $a''$  frequency. Figure 7 shows cross-sections of the MP2/6-31G(d) potential surface for this bending motion at various values of the CNO angle. (The surface was obtained by computing the molecular energies at a range of fixed values of the CNO and dihedral angles, with all other geometric parameters fully optimized at each grid-point at the MP2/6-31G(d) level.) From this diagram it is seen that the bifurcation region on the PES exists for CNO angles ranging from  $\sim 70^\circ$  to  $45^\circ$ . If this  $a''$  mode is followed, i.e., the molecule is allowed to become nonplanar, the product so formed is the higher-energy cyclic N(H)CO ( $^1A$ ) (oxaziridinylidene) isomer rather than HNCO. As before, this reaction also results in the formation of a CO bond but without severance of the NO bond. The lesser stability of cyclic N(H)CO, in relation to the other isomers, is reflected in its geometry where two bonds involving heavy atoms are elongated, namely, NO (1.57 Å) and CN (1.45 Å). Unlike cyclic C(H)NO, the lowest-lying triplet state of cyclic N(H)CO, which again is an open-chain molecule, CN(H)O ( $^3A''$ ), lies far above it (by  $\sim 50$  kcal/mol on the basis of G2 energies).



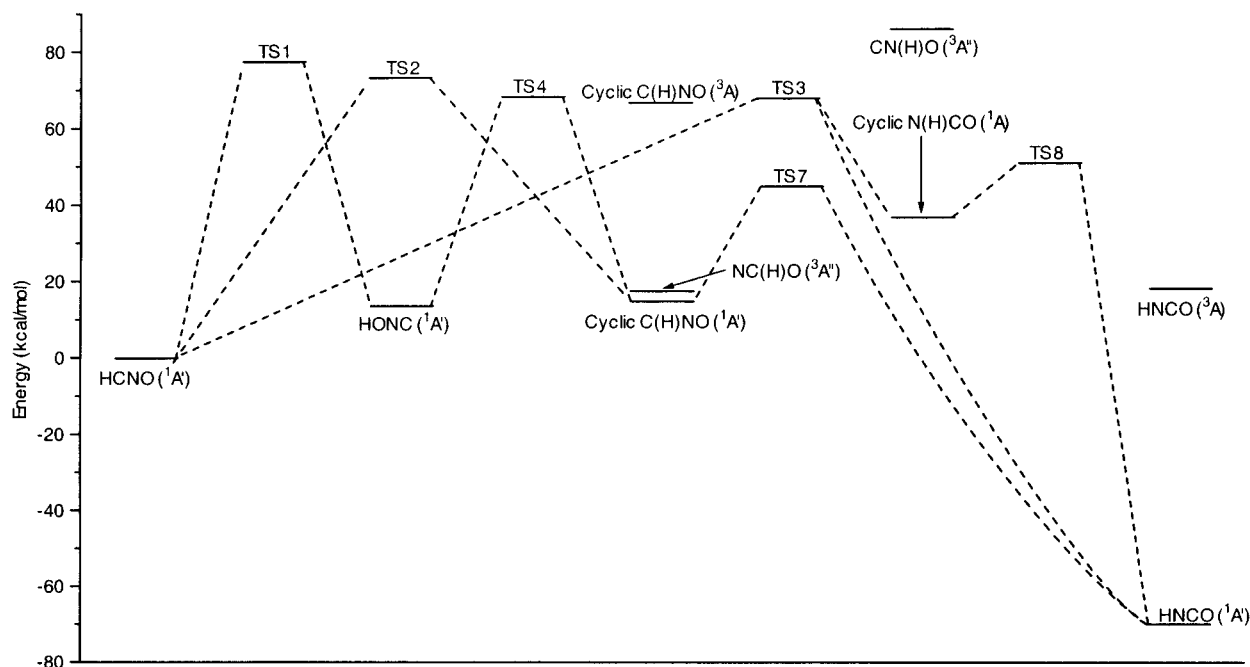


Figure 6. Schematic G2 potential energy surface for HCNO isomerizations.

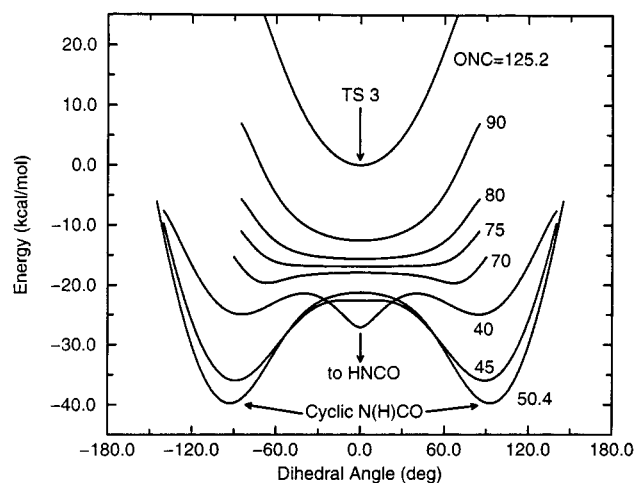


Figure 7. MP2/6-31G(d) out-of-plane distortion potentials at selected CNO angles along the reaction coordinate leading from TS3 to HNCO/Cyclic N(H)CO.

The forward barrier heights for isomerization to HNCO or cyclic N(H)CO are, of course, identical at 67.4 kcal/mol. Because TS3 connects both these species to HCNO, it can also be thought of as a transition state connecting these species to each other (i.e., HNCO to cyclic N(H)CO). It turns out, though, that a lower energy pathway for interconversion of the two exists, as discussed below.

**3. HONC ( $^1A'$ )  $\rightarrow$  Cyclic C(H)NO ( $^1A'$ )/Cyclic O(H)CN ( $^1A'$ )  $\rightarrow$  HOCN ( $^1A'$ ).** The formation of cyclic C(H)NO from HONC is reminiscent of the formation of HCNO from HONC (via TS1) in that both processes involve 1,3-H transfers from O to C. However, in this case the reaction, proceeding through the transition state TS4, also involves the simultaneous formation of a C–O bond. Unlike TS1, the CNO angle in TS4 is quite small at only  $79^\circ$ , allowing close contact between C and O centers in addition to short H–C and H–O bond lengths (relative to those for other 1,3-H shifts in both the CHNO and CH<sub>2</sub>NO systems). As may be expected, TS4 is more stable than TS1 (by  $\sim 10$  kcal/mol). The critical energy for this reaction is thus 53.8 kcal/mol.

HONC may also cyclize via TS5 to the (meta-)stable isomer cyclic O(H)CN ( $^1A'$ ), the PES for which is shown in Figure 8. As might be expected, the ON and OC bonds in this cyclic system are quite elongated (1.57 and 1.73 Å respectively) which is suggestive of a weakly bound molecular complex between OH and CN. It is best described in terms of a bonding interaction between a singly occupied (in-plane)  $\pi$  MO of CN and the singly occupied  $\pi$  MO of OH. This species may readily revert to HONC, with a critical energy of only 0.05 kcal/mol, or isomerize to HOCN via TS6, with a critical energy of 2.6 kcal/mol. Given the small barriers to interconversion at the G2 level, an equilibrium structure for cyclic O(H)CN may not be reproducible at higher (than MP2) levels of theory and the conversion of HONC to HOCN may actually be a one-step process with a cyclic O(H)CN system representing the intervening transition state.

**4. HNCO ( $^1A'$ )  $\rightarrow$  Cyclic C(H)NO ( $^1A'$ )/Cyclic N(H)CO ( $^1A'$ ).** HNCO is predicted to be the most stable of all CHNO isomers. It can cyclize to cyclic C(H)NO and cyclic N(H)CO via TS7 and TS8, respectively. The first of these reactions involves a simple 1,2-H shift from N to C with a concomitant ring closing process that takes place on the ( $^1A'$ ) surface. The critical energy for this process is 114.8 kcal/mol with an endothermicity of 84.9 kcal/mol, although in absolute terms the barrier is fairly low at 44.7 kcal/mol (above HCNO). Using the IRC method (at the MP2/6-31G(d) level of theory) we confirmed that TS7 does indeed directly connect C(H)NO and cyclic N(H)CO. The imaginary frequency ( $777i$  cm<sup>-1</sup> at the MP2/6-31G(d) level) is of  $a'$  symmetry, as expected. Isomerization to cyclic N(H)CO via TS8 involves a rotation of the H around the NC bond as the cyclization occurs and this pathway is energetically more favorable than the alternative discussed above, via TS3. The product formed has a considerably higher energy than cyclic C(H)NO, although the critical energies differ by less than 6 kcal/mol.

**5. HOCN ( $^1A'$ )  $\rightarrow$  HNCO ( $^1A'$ )/Cyclic N(H)CO ( $^1A'$ ).** HOCN may isomerize to HNCO through two different pathways with greatly varying critical energies, although both are 1,3-H transfers that take place on the ( $^1A'$ ) surface. The low-energy route proceeds via TS9 with a critical energy of 62.5 kcal/mol

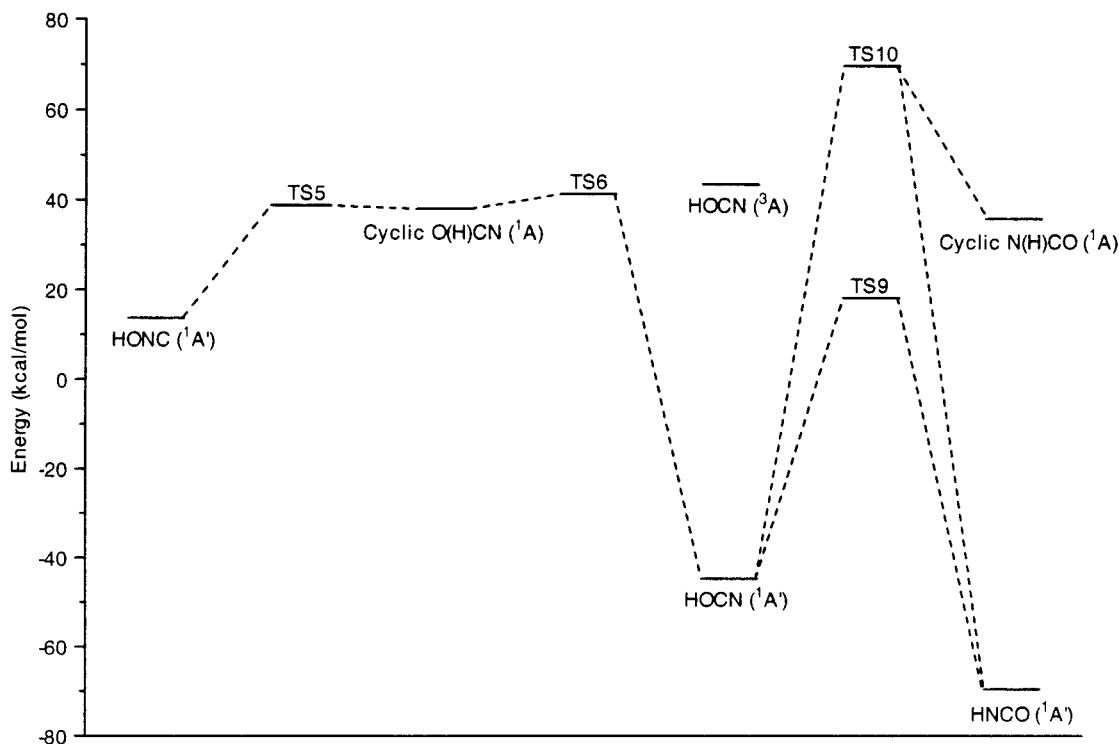


Figure 8. Schematic G2 potential energy surface for HCNO isomerizations. (The energies are relative to HCNO.)

and an exothermicity of 25.4 kcal/mol at 0 K. The geometry of this transition state resembles that of TS1 (which also describes a 1,3-H shift) in that the heavy-atom backbone retains a near linear arrangement, allowing the H to once again stay in close contact with the heavy-atom in the center (in this instance, C). As in the case for TS1, using the IRC method (at the MP2/6-31G(d) level of theory) we confirmed that TS9 connects the above reactant and product, viz. HOCN and HNCO, respectively. Similarly, the imaginary frequency ( $1744i \text{ cm}^{-1}$  at the MP2/6-31G(d) level) is of  $a'$  symmetry. The alternative high-energy route via TS10 is associated with a critical energy of 114.5 kcal/mol. In this structure, where the NCO angle (of  $75^\circ$ ) is considerably smaller than in TS9, the contact between H and C is now nonexistent, although the HN and HO lengths are shorter. Evidently the stabilization afforded by stronger bonding of H with the N and O centers does not make up for the energy penalty incurred by breaking the HC bond and bending the NCO framework. It is worth noting that TS9 and TS10 have the same electron configurations, each with four electrons in  $a''$  MOs.

TS10 also connects HOCN with cyclic N(H)CO (in much the same way that TS3 connects HCNO with both HNCO and cyclic N(H)CO). On going from HOCN to TS10 the system retains its planarity; however, for a certain region on the product side of the PES the potential is actually a maximum with respect to out-of-plane distortions of the H atom, i.e., the planar structure possesses an imaginary  $a''$  frequency. (A plot of cross-sections of the PES in the region  $\text{TS10} \rightarrow \text{HNCO/cyclic N(H)CO}$  shows the same essential features as those of Figure 7 for the PES in the region  $\text{TS3} \rightarrow \text{HNCO/cyclic N(H)CO}$  and, therefore, it is not reproduced here). If this  $a''$  mode is followed, the product formed is cyclic N(H)CO rather than the planar HNCO.

**6.  $\text{HCNO} ({}^1A')$   $\rightarrow$   $\text{HC} + \text{NO}$  and  $\text{HOCN} ({}^1A')$   $\rightarrow$   $\text{HO} + \text{CN}$ .** These two dissociations proceed in a straightforward manner with simple bond fissions. HCNO dissociates via TS11 to yield the ground-state products  $\text{HC} ({}^2\Pi) + \text{NO} ({}^2\Pi)$  with an associated endothermicity of 120.8 kcal/mol. In contrast with the MP2 calculations that located a transition state geometry

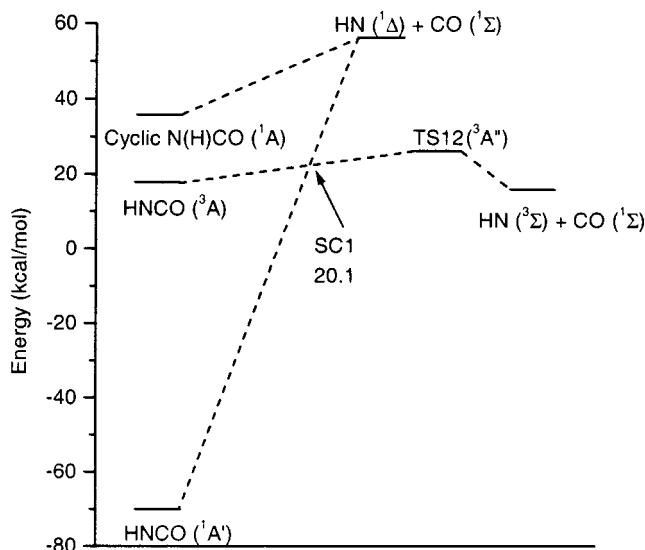


Figure 9. Schematic G2 potential energy surface for HNCO and Cyclic N(H)CO dissociation. (The energies are relative to HCNO.)

for TS11, subsequent CASSCF calculations (carried out using the DALTON codes<sup>23</sup> with 10 active electrons in 10 active orbitals in Dunning's cc-pVDZ basis<sup>19</sup>) failed to find a first-order saddle point. Thus the reverse association is most likely barrierless, TS11 (with an extremely long CN distance of  $\sim 2.7 \text{ \AA}$ ) being simply an artifact of the MP2 computations. HOCN dissociates to the ground-state products  $\text{HO} ({}^2\Pi) + \text{CN} ({}^2\Sigma)$  with an endothermicity of 74.3 kcal/mol. Once again, a transition state structure (TS13) was located at the MP2 level, but could not be reproduced when the CASSCF method was used, as described above. Thus the recombination of HO and CN is likely also to be barrierless.

**7.  $\text{HNCO} ({}^1A')$   $\rightarrow$   $\text{HN} + \text{CO}$  and  $\text{Cyclic N(H)CO} ({}^1A')$   $\rightarrow$   $\text{HN} + \text{CO}$ .** The dissociation of HNCO, for which the schematic G2 PES is depicted in Figure 9, is a little more complex than

**TABLE 2: QCISD(T) and B3LYP Electronic Energies of the Selected Isomers and Transition States Associated with the Isomerization and Dissociation Reactions of HCNO<sup>a</sup>**

	QCISD(T) cc-pVTZ ( <i>E<sub>h</sub></i> )	B3LYP cc-pVTZ ( <i>E<sub>h</sub></i> )	B3LYP 6-311G(d,p) ( <i>E<sub>h</sub></i> )
HCNO ( <sup>1</sup> A')	-168.322434	-168.638700	-168.619814
HONC ( <sup>1</sup> A')	-168.301703	-168.611526	-168.592238
TS2 ( <sup>1</sup> A')	-168.204833	-168.524480	-168.504426
Cyclic C(H)NO ( <sup>1</sup> A')	-168.296548	-168.603286	-168.583303
Cyclic C(H)NO ( <sup>3</sup> A)	-168.221183	-168.536543	-168.517714
HNCO ( <sup>1</sup> A')	-168.433654	-168.750385	-168.732021
HNCO ( <sup>3</sup> A)	-168.296222	-168.614683	-168.596886
Cyclic N(H)CO ( <sup>1</sup> A)	-168.265880	-168.571709	-168.551913
CN(H)O ( <sup>3</sup> A'')	-168.191064	-168.512371	-168.494613
TS4 ( <sup>1</sup> A')	-168.210666	-168.514873	-168.495368
HOCN ( <sup>1</sup> A')	-168.395162	-168.704139	-168.685751
TS8 ( <sup>1</sup> A)	-168.238764	-168.543826	-168.525100
TS10 ( <sup>1</sup> A)	-168.206856	-168.512297	-168.492960
TS12 ( <sup>3</sup> A')	-168.282854	-168.596802	-168.580103
HC ( <sup>2</sup> Π) + NO ( <sup>2</sup> Π)	-168.127932	-168.436747	-168.418584
HN ( <sup>3</sup> Σ) + CO ( <sup>1</sup> Σ)	-168.296794	-168.598819	-168.582106
HO ( <sup>2</sup> Π) + CN ( <sup>2</sup> Σ)	-168.202717	-168.508210	-168.489317
HNOC ( <sup>1</sup> A')	-168.218253	-168.532856	-168.512598

<sup>a</sup> At MP2/6-31G(d) geometry.

that of HCNO and HOCN. In this instance the (<sup>1</sup>A') ground state of HNCO correlates with an excited state of HN, giving a heat of reaction (at 0 K) for production of HN (<sup>1</sup>Δ) + CO (<sup>1</sup>Σ) of 126.5 kcal/mol, with no reverse barrier. However, the first (<sup>3</sup>A) excited state of HNCO does correlate with the ground-state products. The equilibrium structure for this state of HNCO contains an elongated NC bond, 1.43 Å, to be compared with 1.22 Å in the ground state. Consequently, the critical energy required to break this bond is rather small at only 8.6 kcal/mol. As the reaction proceeds the molecule assumes a planar geometry, so that the transition state TS12 is a <sup>3</sup>A'' state, leading to HN (<sup>3</sup>Σ) + CO (<sup>1</sup>Σ). The minimum energy path (MEP) for dissociation from ground-state HNCO to ground-state products therefore necessitates a crossing from the <sup>1</sup>A' to the <sup>3</sup>A'' surface. As Mebel et al.<sup>1</sup> located the geometry of this intersystem crossing (SC1) (by minimization of the crossing seam by the constrained optimization method of Koga and Morokuma<sup>24</sup>) at the MP2/6-311G(d,p) level, we utilized their geometry to obtain a G2 estimate of the energy of SC1. The resulting G2 triplet and singlet electronic energies were found to agree to within

0.4 kcal/mol, provided the higher level corrections were excluded. With the inclusion of zero point energy corrections (obtained at the MP2 level, with the appropriate projection applied to the SC1 Hessian<sup>25,26</sup>) the energy of SC1 (computed for the triplet state) was found to be 2.4 kcal/mol above the equilibrium energy of HNCO (<sup>3</sup>A), viz. 20.1 kcal/mol above HCNO (<sup>1</sup>A'). Given that SC1 is located before the transition state TS12 on the PES, the energy of the latter defines the critical energy for the dissociation of HNCO, viz. 96.4 kcal/mol, with an endothermicity of 86.0 kcal/mol. Use of the B3LYP/6-311G-(d,p) geometry of Mebel et al.<sup>1</sup> for SC1 yields a G2 estimate of its energy that is ~1.5 kcal/mol lower than at the above MP2 geometry, although in this case the singlet and triplet G2 electronic energies differ by 7.3 kcal/mol.

Cyclic N(H)CO was also determined to dissociate directly to HN (<sup>1</sup>Δ) + CO (<sup>1</sup>Σ). No saddle point was found for this process, indicating that the recombination may be barrierless. The small G2 reaction enthalpy (at 0 K) of 20.6 kcal/mol is in line with the weak interaction between HN and CO as evident also from the elongated NC and NO bonds of the cyclic isomer. With the exception of the "unusual" cyclic O(H)CN isomer (and HNOC and HCON), cyclic N(H)CO has the highest energy and the smallest barriers to isomerization/decomposition of all the species considered in this paper. On the basis of the G2 results, its formation in appreciable quantities in combustion systems is therefore expected to be minimal.

**Comparison of G2, QCISD(T), and DFT Energies.** Further calculations were performed in an effort to elucidate the reasons for the observed differences in the G2 and B3LYP/6-311G-(d,p) energies (as computed by Mebel et al.<sup>1</sup>) of the isomers and transition states common to the studies by both these authors and by us. To this end, QCISD(T) and B3LYP energies, employing the cc-pVTZ basis, and B3LYP/6-311G(d,p) energies were computed for these species at their MP2/6-31G(d) geometries. These absolute energies are listed in Table 2 whereas energies relative to HCNO, along with those of Mebel et al., are listed in Table 3.

An examination of the G2 and QCI energies presented in Table 3 reveals close agreement, generally within ~2 kcal/mol of each other, with the exception of the triplet species cyclic C(H)NO (<sup>3</sup>A), HNCO (<sup>3</sup>A), CN(H)O (<sup>3</sup>A''), and TS12 (<sup>3</sup>A') where the G2 energy is ~3–4.5 kcal/mol higher than the QCI value. However, as noted by Sendt et al.,<sup>27</sup> G2 seems to

**TABLE 3: G2, QCISD(T), and B3LYP Relative (to HCNO) Energies (in kcal/mol) of Selected Isomers and Transition States Associated with the Isomerization and Dissociation Reactions of HCNO, Computed at MP2/6-31G(d) Geometries unless Indicated Otherwise**

	G2 <sup>a</sup>	QCISD(T) cc-pVTZ <sup>a</sup>	B3LYP cc-pVTZ <sup>a</sup>	B3LYP 6-311G(d,p) <sup>a</sup>	B3LYP 6-311G(d,p) <sup>b</sup>
HONC ( <sup>1</sup> A')	13.7	12.7	16.7	17.0	19.2
TS2 ( <sup>1</sup> A')	73.2	71.2	69.1	69.8	69.8
Cyclic C(H)NO ( <sup>1</sup> A')	14.8 <sup>c</sup>	15.1 <sup>c</sup>	21.1 <sup>c</sup>	21.7 <sup>c</sup>	24.0
Cyclic C(H)NO ( <sup>3</sup> A)	66.4	62.6	63.2	63.1	65.6
HNCO ( <sup>1</sup> A')	-70.1	-69.9	-70.2	-70.5	-67.9
HNCO ( <sup>3</sup> A)	17.7	14.5	13.2	12.5	14.7
Cyclic N(H)CO ( <sup>1</sup> A)	35.9	34.9	41.4	42.0	44.4
CN(H)O ( <sup>3</sup> A'')	85.7	81.4	78.2	77.5	80.1
TS4 ( <sup>1</sup> A')	67.6	66.1	73.7	74.1	77.4
HOCN ( <sup>1</sup> A')	-44.7	-45.3	-40.8	-41.1	-39.2
TS8 ( <sup>1</sup> A)	50.1	49.8	56.8	56.7	55.8
TS10 ( <sup>1</sup> A')	69.9	67.8	74.6	74.9	78.0
TS12 ( <sup>3</sup> A')	26.3	21.7	23.1	21.7	24.8
HC ( <sup>2</sup> Π) + NO ( <sup>2</sup> Π)	120.8	119.9	124.6	124.1	122.8
HN ( <sup>3</sup> Σ) + CO ( <sup>1</sup> Σ)	15.9	15.4	24.3	22.9	20.4
HO ( <sup>2</sup> Π) + CN ( <sup>2</sup> Σ)	74.3	74.4	81.2	81.2	78.7
HNOC ( <sup>1</sup> A')	62.0 <sup>c</sup>	62.6 <sup>c</sup>	63.6 <sup>c</sup>	64.5 <sup>c</sup>	67.1

<sup>a</sup> Using Δ*E*<sub>ZPE</sub>(G2). <sup>b</sup> Results of Mebel et al.<sup>1</sup> (at B3LYP/6-311G(d,p) geometry). <sup>c</sup> Using scaled MP2 frequencies.

underestimate the stability of triplet states by  $\sim 2.5$  kcal/mol. If this is taken into account, the "corrected" G2 energy of these triplet species will fall within  $\sim 2$  kcal/mol of the QCI value, in line with the other species considered in Table 3.

A comparison of the B3LYP/6-311G(d,p) energies computed at the MP2 and B3LYP geometries allows a quantification to be made as to the effect of equilibrium geometry on the energetics. With the exception of TS2, the differences between the two sets of results are consistently around 2–3 kcal/mol. The basis set effects, examined by comparing the B3LYP/6-311G(d,p)/MP2/6-31G(d) and B3LYP/cc-pVTZ//MP2/6-31G(d) energies, are quite small. However, on comparing the QCISD(T) and B3LYP energies obtained with the cc-pVTZ basis (at MP2 geometries), it is evident that the differences in the relative energies as predicted by these two methods are generally much larger than those due to different basis sets or different geometries and may be as large as  $\sim 9$  kcal/mol, as in the case of HN + CO. Overall, therefore, the discrepancy between the G2 (and/or QCI) and the DFT energies of Mebel et al. are mostly due to the implicit differences between the G2/QCI and B3LYP methodologies, whereas the differences in geometries are considerably less important. Given the demonstrated reliability of the G2 method,<sup>12,16–18</sup> and also the close agreement with the QCI/cc-pVTZ results reported here, the G2 results are expected to be more reliable, with the proviso that the energy of triplet state molecules is suitably adjusted to account for its deficiencies in the area of singlet/triplet splittings.

## Conclusion

The ab initio quantum chemical study discussed in this work examined the potential energy surface associated with the HCNO system, identifying a number of possible routes for isomerization and decomposition. Isomerizations can occur by direct 1,3-H shifts, as well as via cyclic intermediates. The latter represent the lower energy pathways. The four open-chain isomers possessing CNO and NCO backbones were found to have the lowest energies, with isocyanic acid (HNCO) being the most stable. Two stable cyclic isomers, C(H)NO and N(H)CO, were also characterized, as was the meta-stable cyclic O(H)CN isomer. In general, several pathways can lead to the formation of a given isomer. Most notably, two bifurcation points were found on the PES. The first occurs on the reaction path that connects HCNO with both HNCO and cyclic N(H)CO, once the transition state TS3 is passed; the second connects HOCN (via TS10) with HNCO and cyclic N(H)CO.

Comparison of the G2 and DFT energies for a range of isomers and transition states indicates that while a reasonable level of agreement between the two approaches can be demonstrated, the discrepancies can be unexpectedly large,  $\sim 9$  kcal/mol in the computed energy of reaction.

**Acknowledgment.** The award of a Sydney University Postgraduate Scholarship to W.A.S. is gratefully acknowledged.

## References and Notes

- (1) Mebel, A. M.; Luna, A.; Lin, M. C.; Morokuma, K. *J. Chem. Phys.* **1996**, *105*, 6439.
- (2) East, A. L. L.; Johnson, C. S.; Allen, W. D. *J. Chem. Phys.* **1993**, *98*, 1299.
- (3) Pinnavaia, N.; Bramley, M. J.; Su, M.-D.; Green, W. H.; Handy, N. C. *Mol. Phys.* **1993**, *78*, 319.
- (4) Yokoyama, K.; Takane, S.-Y.; Fueno, T. *Bull. Chem. Soc. Jpn.* **1991**, *64*, 2230.
- (5) Poppinger, D.; Radom, L.; Pople, J. A. *J. Am. Chem. Soc.* **1977**, *99*, 7806.
- (6) Miller, J. A.; Bowman, C. T. *Prog. Energy Combust. Sci.* **1989**, *15*, 287 and references therein.
- (7) Wendt, J. O. L.; Sternling, C. V.; Matovich, M. A. *14th Symposium (International) on Combustion*; The Combustion Institute: Pittsburgh, 1973; p 897.
- (8) Myerson, A. L. *15th Symposium (International) on Combustion*; The Combustion Institute: Pittsburgh, 1975; p 1085.
- (9) Song, Y. H.; Blair, D. W.; Siminski, V. J.; Bartok, W. *18th Symposium (International) on Combustion*; The Combustion Institute: Pittsburgh, 1981; p 53.
- (10) Chen, S. L.; McCarthy, J. M.; Clark, W. D.; Heap, M. P.; Seeker, W. R.; Pershing, D. W. *21st Symposium (International) on Combustion*; The Combustion Institute: Pittsburgh, 1986; p 1159.
- (11) Perry, R. A.; Siebers, D. L. *Nature (London)* **1986**, *324*, 657.
- (12) Shapley, W. A.; Bacskay, G. B. *Theor. Chem. Acc.* **1998**, *100*, 212.
- (13) Atakan, B.; Kocis, D.; Wolfrum, J.; Nelson, P. *24th Symposium (International) on Combustion*; The Combustion Institute: Pittsburgh, 1992; p 691.
- (14) Roggenbuck, J.; Temps, F. *Chem. Phys. Lett.* **1998**, *285*, 422.
- (15) Grussdorf, J.; Temps, F.; Wagner, H. Gg. *Ber. Bunsen-Ges. Phys. Chem.* **1997**, *101*, 134.
- (16) Shapley, W. A.; Bacskay, G. B. *J. Phys. Chem. A* **1999**, *103*, 4505.
- (17) Shapley, W. A.; Bacskay, G. B. *J. Phys. Chem. A* **1999**, *103*, 4514.
- (18) Curtiss, L.; Raghavachari, K.; Trucks, G.; Pople, J. *J. Chem. Phys.* **1991**, *94*, 7221.
- (19) Dunning, T. H. *J. Chem. Phys.* **1989**, *90*, 1007.
- (20) Frisch, M. J.; Trucks, G. W.; Schlegel, H. B.; Gill, P. M. W.; Johnson, B. G.; Robb, M. A.; Cheeseman, J. R.; Keith, T.; Petersson, G. A.; Montgomery, J. A.; Raghavachari, K.; Al-Laham, M. A.; Zakrzewski, V. G.; Ortiz, J. V.; Foresman, J. B.; Peng, C. Y.; Ayala, P. Y.; Chen, W.; Wong, M. W.; Andres, J. L.; Replogle, E. S.; Gomperts, R.; Martin, R. L.; Fox, D. J.; Binkley, J. S.; Defrees, D. J.; Baker, J.; Stewart, J. P.; Head-Gordon, M.; Gonzalez, C.; Pople, J. A. *Gaussian 94 (Revision B.3)*; Gaussian, Inc.: Pittsburgh, PA, 1995.
- (21) Koput, J.; Winnewisser, B. P.; Winnewisser, M. *Chem. Phys. Lett.* **1996**, *255*, 357.
- (22) Rendell, A. P.; Lee, T. J.; Lindh, R. *Chem. Phys. Lett.* **1992**, *194*, 84.
- (23) DALTON Release 1.0 1997 is an ab initio electronic structure program, written by T. Helgaker, H. J. Å. Jensen, P. Jørgensen, J. Olsen, K. Ruud, H. Ågren, T. Anderson, K. L. Bak, V. Bakken, O. Christiansen, P. Dahle, E. K. Dalskov, T. Enevoldsen, B. Fernandez, H. Heiberg, H. Hettema, D. Jonsson, S. Kirpekar, R. Kobayashi, H. Koch, K. V. Mikkelsen, P. Norman, M. J. Packer, T. Saue, P. R. Taylor, O. Vahtras.
- (24) Koga, N.; Morokuma, K. *Chem. Phys. Lett.* **1985**, *119*, 371.
- (25) Miller, W. H.; Handy, N. C.; Adams, J. E. *J. Chem. Phys.* **1980**, *72*, 99.
- (26) CADPADC 6.0: The Cambridge Analytical Derivatives Package Issue 6, Cambridge, 1995. A suite of quantum chemistry programs developed by R. D. Amos with contributions from I. L. Alberts, J. S. Andrews, S. M. Colwell, N. C. Handy, D. Jayatilaka, P. J. Knowles, R. Kobayashi, K. E. Laidig, G. Laming, A. M. Lee, P. E. Maslen, C. W. Murray, J. E. Rice, E. D. Simandiras, A. J. Stone, M.-D. Su, D. J. Tozer.
- (27) Sendt, K.; Ikeda, E.; Bacskay, G. B.; Mackie, J. C. *J. Phys. Chem. A* **1999**, *103*, 1054.